scientific reports

Check for updates

OPEN

Characterization and utility of two monoclonal antibodies to cholera toxin B subunit

Noel Verjan Garcia[1], Ian Carlosalberto Santisteban Celis[2], Matthew Dent[3] & Nobuyuki Matoba[1,2,3]✉

Cholera toxin B subunit (CTB) is a potent immunomodulator exploitable in mucosal vaccine and immunotherapeutic development. To aid in the characterization of pleiotropic biological functions of CTB and its variants, we generated a panel of anti-CTB monoclonal antibodies (mAbs). By ELISA and surface plasmon resonance, two mAbs, 7A12B3 and 9F9C7, were analyzed for their binding affinities to cholera holotoxin (CTX), CTB, and EPICERTIN: a recombinant CTB variant possessing mucosal healing activity. Both 7A12B3 and 9F9C7 bound efficiently to CTX, CTB, and EPICERTIN with equilibrium dissociation constants at low to sub-nanomolar concentrations but bound weakly, if at all, to *Escherichia coli* heat-labile enterotoxin B subunit. In a cyclic adenosine monophosphate assay using Caco2 human colon epithelial cells, the 7A12B3 mAb was found to be a potent inhibitor of CTX, whereas 9F9C7 had relatively weak inhibitory activity. Meanwhile, the 9F9C7 mAb effectively detected CTB and EPICERTIN bound to the surface of Caco2 cells and mouse spleen leukocytes by flow cytometry. Using 9F9C7 in immunohistochemistry, we confirmed the preferential localization of EPICERTIN in colon crypts following oral administration of the protein in mice. Collectively, these mAbs provide valuable tools to investigate the biological functions and preclinical development of CTB variants.

Cholera toxin B subunit (CTB, approx. 58 kDa), is a nontoxic component of the cholera toxin (CTX) released by *Vibrio cholerae*, a Gram-negative bacterium causing profuse secretory diarrhea[1]. CTB is a potent immunomodulator consisting of five identical polypeptide chains non-covalently associated in a ring-shaped pentameric structure that mediates CTX binding to the monosialoganglioside GM1 receptor[2–4]. CTB has been produced in various recombinant expression platforms as model vaccines[5–8], as it induces a strong immune response characterized by neutralizing antibodies to the CTX via oral administration[9,10]. CTB has also been used as a molecular scaffold for immunization[11,12] and for induction of peripheral (oral) immunological tolerance to suppress allergies and various autoimmune disorders such as experimental autoimmune encephalitis (EAE), diabetes, arthritis and uveitis in an antigen-specific manner[13–17]. CTB is considered a mucosal immunomodulator that induces a strong mucosal IgA response while it seems to suppress systemic T helper (T_H1, T_H2 and T_H17) responses through the induction of interleukin-10 (IL-10) and transforming growth factor-β (TGF-β)-mediated regulatory T (Treg) cell induction and suppression of proinflammatory IL-6[18], although the exact mechanism behind such immunomodulation remains elusive.

The pleiotropic functions of CTB have recently been expanded through the construction of CTB variants with novel biological activities, including a plant-made CTB variant modified with C-terminal hexapeptide extension containing a KDEL endoplasmic reticulum (ER) retention motif[19], later designated as EPICERTIN[20], which showed a significant enhancement of mucosal wound healing activity in the colon[21–25]. In mice, oral administration of EPICERTIN increased specific subsets of immune cell populations, such as macrophages, natural killer cells, Treg cells and T_H17 cells in the colon lamina propria and upregulated wound healing pathway genes mediated by TGF-β in the colon. Mucosal healing effects of EPICERTIN were confirmed in an in vivo dextran sodium sulfate (DSS) acute colitis model, an azoxymethane/DSS model of ulcerative colitis and tumorigenicity[21], and a model of chronic colitis-like colon inflammation induced by repeated doses of DSS, where the wound healing effects were not neutralized by the induction of mucosal anti-CTB antibodies[24]. The prolonged residence of EPICERTIN in the ER, through interaction with the KDEL receptor, appears to trigger an unfolded protein

[1]UofL Health – Brown Cancer Center, University of Louisville School of Medicine, Louisville, KY, USA. [2]Center for Predictive Medicine, University of Louisville School of Medicine, 505 S. Hancock Street, Room 615, Louisville, KY 40202, USA. [3]Department of Pharmacology and Toxicology, University of Louisville School of Medicine, Louisville, KY, USA. ✉email: n.matoba@louisville.edu

response, which leads to the activation of TGF-β signaling and transcription of wound healing pathway genes in colon epithelial cells[23]. However, the mucosal healing effects could also originate from modulation of mucosal immune cells. Indeed, early studies reported multiples roles of CTX and CTB in mouse and human leukocytes. For example, CTB inhibited T-cell proliferation induced by mitogens (e.g. Concanavalin A) and antigens[26], and antigen-conjugated CTB promoted its presentation and lowered the threshold of antigen required for T cell activation[27]. Therefore, to facilitate the investigation of the mechanisms behind the biological activities of EPICERTIN and other CTB-derived molecules, we aimed at characterizing two monoclonal antibodies (mAbs) that were generated against CTB to aid in the study of those proteins.

Here, we report on the isolation and characterization of two mAbs, 7A12B3 and 9F9C7, that were generated against CTB, demonstrating their unique and distinct binding profiles by means of ELISA, surface plasmon resonance (SPR)[28] and cyclic adenosine monophosphate (cAMP) assays. In addition, we show the utility of these mAbs in neutralizing CTX and detecting CTB bound both to murine leukocytes by flow cytometry and to colon tissues by immunohistochemistry (IHC). Together with our previous studies that utilized these mAbs in immunofluorescence, immunoprecipitation and pharmacokinetic analyses of EPICERTIN[20,23], the present study underscores that 7A12B3 and 9F9C7 will aid in investigating as-yet-uncharacterized biological mechanisms of action of CTB and its derivatives as candidate mucosal vaccines and immunotherapeutics.

Methods

Animal care. Immunization of Wistar rats for hybridoma generation was conducted by GenScript USA, Inc. (Piscataway, NJ), whereas flow cytometry and IHC experiments using C57BL/6J mice were performed at the University of Louisville. Studies were approved by each institution's Institutional Animal Care and Use Committee and are reported in compliance with the ARRIVE guidelines. General procedures for animal care and housing in these studies were in accordance with the current Association for Assessment and Accreditation of Laboratory Animal Care recommendations, current requirements stated in the Guide for the Care and Use of Laboratory Animals (National Research Council), and current requirements as stated by the U.S. Department of Agriculture through the Animal Welfare Act and Animal Welfare regulations (July 2020).

Reagents. Cholera enterotoxin (C8052), cholera toxin B-subunit (CTB; C9903) and heat labile enterotoxin B subunit (LTB; E9656) of *Escherichia coli* were purchased from Sigma (Sigma Aldrich). PhenoVue Fluor 594-WGA was obtained from PerkinElmer (Perkin Elmer Health Science Inc. Boston MA, USA), and Alexa Fluor 647-conjugated rat anti mouse/human CD324 (E-cadherin) (clone DECMA-1) was obtained from Biolegend.

Generation of anti-CTB mAbs. To facilitate the generation of CTX-neutralizing mAbs, an Asn4-glycosylated CTB variant produced in *Nicotiana benthamiana*[19,29] (gCTB) was used as an antigen for immunization. The plant-expressed gCTB was purified by metal-affinity chromatography followed by CHT hydroxyapatite chromatography, as described previously[19]. The purified protein was used to immunize Wistar rats to generate a panel of monoclonal antibodies by Genscript USA, Inc. using standard hybridoma technology[30,31]. Briefly, three Wistar rats were immunized with 50 µg of keyhole limpet hemocyanin conjugated gCTB (gCTB-KLH) and subsequently boosted with 25 µg gCTB-KLH every two weeks, for a total of three booster doses. Two weeks after the last booster immunization, the lymphocyte population from spleens were isolated and used to generate immortalized hybridomas by fusion with the Sp2/0-Ag14 myeloma cells following standard methods. Hybridomas were grown in Hypoxanthine-aminopterin-thymidine medium supplemented with IL-6, and the culture supernatants were screened for Abs reactive with CTB by antigen-capture enzyme-linked immunosorbent assay (ELISA) and GM1-capture ELISA. Two anti-CTB mAbs-producing hybridomas named 7A12B3 and 9F9C7 were selected and expanded, and mAbs were produced in hybridoma cell culture supernatants using the invitro roller bottle cell culture method followed by protein G-affinity chromatography purification. They were both determined to be of the IgG2a subclass by using the Pro-Detect™ Rapid Antibody Isotyping Kit- Rat (Thermo Fisher Scientific).

Enzyme-linked immunosorbent assays. Binding affinities of 7A12B3 and 9F9C7 mAbs to CTX were determined by antigen (CTX, CTB, LTB)-capture ELISA, GM1-capture ELISA, and competitive GM1-capture KDEL-detection (GM1/KDEL) ELISA as described previously[22] with minor modifications as follows:

Antigen-capture ELISA. Ninety-six-well ELISA plates (Nunc, MaxiSorp) were coated with 100 µL per well of 2 µg/mL CTB, CTX or LTB in phosphate-buffered saline (PBS) and incubated at 4 °C overnight. The plates were washed 3 times with PBST (PBS + 0.05% Tween 20) and blocked with 150 µL/well of blocking solution (5% non-fat dry milk in PBST) for 1 h at room temperature. A total of 100 µL/well of serially diluted hybridoma supernatants starting at 1:100 dilution, or purified 7A12B3 and 9F9C7 mAbs diluted in 1% PBST (PBST containing 1% non-fat dry milk) were added after washing 3 times with PBST and incubated at room temperature for 2 h. After 3 washes with PBST, a horseradish peroxidase (HRP)-conjugated goat anti-rat IgG-H&L antibody (SouthernBiotech, Birmingham AL, USA) diluted at 1:5000 was added and incubated at room temperature for 1 h. The plates were washed 3 times and the enzyme substrate tetramethylbenzidine (TMB, 100 µL/well) was added and incubated for 2–3 min at room temperature before stopping the reaction with 100 µl/well of 0.6 N H_2SO_4 stop solution. Absorbance at 450 nm was measured using a BioTek Synergy HT microplate reader (Winooski, VT, USA).

GM1-capture ELISA. ELISA plates were coated with 100 µL per well of 2 µg/mL monoganglioside GM1 (SIGMA-Aldrich) diluted in PBS. After 2-h incubation at room temperature, the plates were washed three times

with PBST and blocked with 150 µL/well of blocking solution for overnight (12–16 h) at 4 °C. The plates were washed 3 × with PBST and a fixed concentration (0.3 µg/mL) of CTB in 1% PBSTM was applied to the plates and incubated at room temperature for 2 h. After washing with PBST, dilutions of hybridomas supernatants or purified mAbs in 1% PBSTM were added and the bound antibodies were detected as described above.

GM1/KDEL ELISA. ELISA plates were coated with GM1 and blocked as described above. After washing the plates 3 times with PBST, 50 µL/well of mAbs at 0, 0.1, 0.3 or 1 µg/mL and 50 µL/well of 2-fold serially diluted EPICERTIN (starting from 2 µg/mL), both prepared in 1% PBSTM, were simultaneously added to plates and incubated at room temperature for 2 h. After washing with PBST, 100 µL/well of mouse anti-KDEL mAb (Enzo LifeSciences; Farmingdale, NY, USA) diluted 1:1000 in 1% PBSTM was added, and plates were incubated at room temperature for 1 h. Plates were washed and goat anti-mouse IgG-HRP (SouthernBiotech) diluted 1:5000 in 1% PBSTM was added, followed by incubation at room temperature for 1 h. After washing 3 times with PBST, the HRP enzyme activity was measured as described above.

Competitive GM1/KDEL ELISA. ELISA plates were coated with GM1, blocked, and washed as described above. Separately, equal volumes of 2-fold serially diluted mAbs (starting from 8 µg/mL) and EPICERTIN at a fixed concentration (0.2 µg/mL), both prepared in 1% PBSTM, were mixed and incubated at room temperature for 30 min in a non-binding round-bottom plate. Then, mAb-EPICERTIN mixtures were added to the GM1-coated plates (100 µL/well), followed by incubation at room temperature for 2 h. The plate-bound EPICERTIN was detected as described above.

Surface plasmon resonance. Binding affinities of 7A12B3 and 9F9C7 mAbs to CTX, commercial CTB, and EPICERTIN were also determined by surface plasmon resonance (SPR) using the Biacore Gold Seal T200 (GE Healthcare) equipped with a CM5 sensor chip as previously described[19]. The ligands 7A12B3 (150 kDa) and 9F9C7 (150 kDa) mAbs were immobilized on the carboxylated dextran matrix of a CM5 chip sensor surface using amine-coupling chemistry. The surfaces of flow cells were activated with a 1:1 mixture of 0.1 M NHS (N-hydroxysuccinimide) and 0.4 M EDC (3-(N,N-dimethylamino) propyl-N-ethylcarbodiimide) at a flow rate of 5 µl/min for 14 min. The ligands at a concentration of 5 µg/ml in 10 mM sodium acetate, pH 4.0, were immobilized at a density of 205–220 RU (7A12B3) and 709 (9F9C7). Flow cells 1 and 3 were left as a reference blank, while flow cells 2 and 4 were used for 7A12B3 and 9F9C7 ligands. Both surfaces were blocked with 1 M ethanolamine, pH 8.0, with a 7 min injection time. Running buffer was 10 mM HEPES, 150 mM NaCl, 0.005% P20, pH 7.4. To collect steady state data and kinetic binding of analytes CTX, CTB, and EPICERTIN to immobilized 7A12B3 mAb, the analytes were diluted to 26.9 nM in running buffer. For 9F9C7 the analytes CTX, CTB, and EPICERTIN were diluted to 1670 nM in running buffer. Samples were 2-fold serially diluted and injected at a flow rate of 10 µL/min and 30 µL/min at 25 °C, respectively. The complexes with 7A12B3 mAb were allowed to associate for 120 s and dissociate for 600 s, whereas the complexes with 9F9C7 mAb were allowed to associate for 180 s and dissociate for 900 s. The surfaces were regenerated with 10 mM Glycine pH 2.0 for 30 s and 60 s for 7A12B3 and 9F9C7 mAbs, respectively. Triplicate injections (in random order) of each sample and a buffer blank were flowed over the two surfaces. Data were collected at a rate of 10 Hz. The data were fit to a Bivalent model using the global data analysis option available within Biacore Evaluation software.

Intracellular cAMP in Caco2 cell line. Caco2 cells were grown in 12-well cluster plates (Thermo Scientific Nunc Cell-Culture Treated, Roskilde, Denmark) at a density of 7×10^5 Caco2 cells/well containing EMEM (Gibco BRL) medium supplemented with 20% FBS, 5 mM HEPES, 5 mM NEAA, 5 mM Sodium Pyruvate and Penicillin/Streptomycin for 24 h. The culture medium was removed, and the cells were washed twice with PBS and then incubated in serum-free EMEM medium containing 2.5 mM HEPES, 0.01% bovine serum albumin, 1 mM 3-Isobutyl-1-methylxanthine (MP Biomedicals, LLC, Solon, Ohio), and the indicated concentrations of 7A12B3 and 9F9C7 mAbs, and 0.5 µg/mL (5.68 nM) of CTX (Sigma, St. Louis, Mo) or rat IgG isotype control for 30 min at 4 °C (on ice). The plates were subsequently transferred to 37 °C in a 5% CO_2 incubator for 2 h. The culture plates were centrifuged at 1000×*g*, the culture medium removed, and the cells washed twice with PBS before incubation in 200 µL of 0.1 N HCl for 20 min at room temperature to allow cell lysis and cAMP extraction[32]. cAMP was detected using a sensitive colorimetric ELISA-based kit (Enzo Life Sciences, Farmingdale, NY) following the manufacturer's conditions. A standard curve was constructed with known concentrations of cAMP and the cAMP levels in the samples (pmol/7×10^5 Caco2 cells) were determined according to the equation generated by the standard curve.

Cell isolation and flow cytometry. C57BL/6J female mice were obtained from Jackson Laboratories (Bar Harbor, ME) and used between 8 and 12-week-old. The spleens of two naïve mice were collected and minced, and the cell suspension passed through a 40 µm cell strainer after treatment with ACK buffer to lyse red cells. The cells were counted, the Fc receptors were blocked with mouse γ-globulins (20 µg/mL), and the cells were subsequently incubated with EPICERTIN or an EPICERTIN variant with Gly33 → Asp mutation (EPICERTIN^{G33D}, [23] 5 µg/mL) for 30 min on ice. After two washes with FACS buffer, unlabeled 9F9C7 mAb was added at 5 µg/mL and the cell suspension incubated on ice for 30 min. Later a FITC-conjugated goat anti-Rat IgG (Poly4054) antibody was added followed by washing and incubation with fluorochrome-labeled antibodies to cell specific markers, including PE-conjugated rat anti-CD4 (RM4-5), PE-conjugated rat anti-IA-IE (M5/114.15.6), PE-conjugated rat anti-Ly6C (Hk1.4), PE-conjugated rat anti-Gr-1 (RB6-8C5), PE or APC-conjugated Armenian Hamster anti-CD11c (N418), APC-conjugated rat anti-CD8a (53-6.7), APC-conjugated rat anti-CD11b (M1/70), APC-conjugated rat anti-Ly6G (1A8), APC-conjugated rat anti-F4/80 (BM8) and PE or APC-conjugated Rat IgG2a

κ isotype control (RTK2758) antibodies, all from Biolegend. APC-conjugated rat anti-CD19 (1D3) was from eBioscience. Flow cytometric analysis was performed on a FACSCalibur or a BD SLRFortessa (BD Biosciences) and the data were processed with FlowJo_v10.8.0_CL software. The geometric mean fluorescence intensity values generated by the goat-anti Rat IgG secondary antibody were subtracted from that of 9F9C7 anti-CTB specific mAb. The procedures with mice were approved by the Institutional Animal Care and Use Committee of University of Louisville.

Immunohistochemistry. EPICERTIN in PBS (3 μg/100μL) was administered by oral gavage to five female C57BL/6 J mice after neutralization of the gastric acid with 200 μL of sodium bicarbonate (30 mg/mL). The mice were sacrificed at 0, 3, 6, 12 or 24 h, and the colon tissues were washed with PBS and embedded in OCT compound to make 7 μm thick frozen sections. Cryosections of the colon tissue were fixed in 100% Methanol at − 20 °C for 3 min, dried and blocked with 10% FBS in PBS containing 20 μg/mL mouse γ-globulins for 1 h at RT. The tissue sections were stained with 5 μg/mL Pheno Vue Fluor 594-WGA (PerkinElmer Health Sciences), 2 μg/mL anti-E-cadherin, and 2 μg/mL anti-CTB (9F9C7 mAb) for 1 h at RT. The slides were washed in PBS, images were collected with a Nikon A1R Confocal laser scanning microscope using 20 × and 60 × magnification lenses with appropriate channels, and the data were processed with the NIS Elements imaging software.

Data analysis. The half-maximal effective concentration (EC_{50}) values were determined by non-linear regression analysis using Prism v.9.1.0. One-way ANOVA with Bonferroni's multiple comparison posttest was used to analyze absorbance values of cAMP levels, using Prism v.9.1.0 (GraphPad Software, La Jolla, CA, USA). A value of $p < 0.05$ was considered significant.

Results

Generation of anti-CTB mAbs. Three Wistar rats were immunized with a KLH-conjugated gCTB. All rats consistently showed high anti-CTB serum antibody titers after three doses of the antigen, as analyzed by both CTB antigen-capture ELISA and GM1-capture ELISA. Given that rat #1 showed an optimal response ratio for direct vs. GM1-bound CTB at a higher dilution factor (1:243,000), indicative of a significant proportion of antibodies targeting the GM1-binding facet of CTB, this rat was selected for hybridoma generation. A total of 40 positive hybridoma clones were obtained. Hybridoma supernatants were analyzed for the presence of anti-CTB antibodies by GM1-capture and CTB antigen-capture ELISAs (Fig. 1A). At this stage, the 7A12, 8F8 and 9F9 hybridomas were initially selected based on the high binding affinity to immobilized CTB in antigen-capture ELISA and in GM1-capture ELISA. Of note, among the three hybridomas, 7A12 and 9F9 mAbs showed very distinctive CTB-binding patterns in ELISA (Fig. 1B), where the binding signal of 7A12 mAb was almost completely abolished in GM1-capture ELISA whereas 9F9 mAb showed similar binding responses regardless of the ELISA formats. Thus, we proceeded with subculturing of these two hybridomas under limiting dilution conditions to

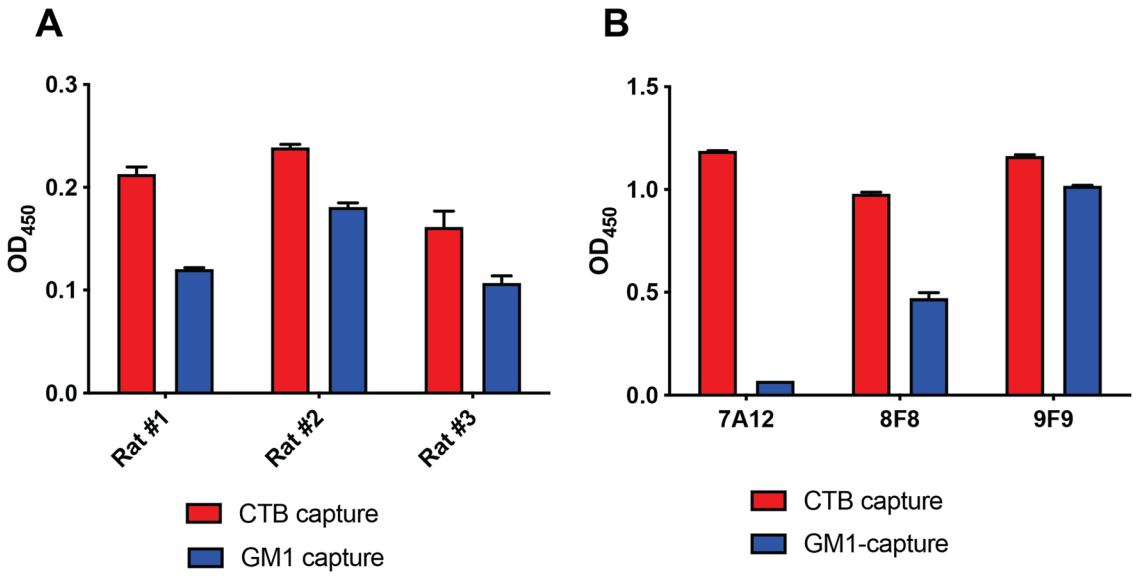

Figure 1. Generation and screening of hybridoma supernatants reacting to CTB. (**A**) Three Wistar rats were immunized with gCTB to generate a panel of mAbs and blood serum from each rat was diluted and analyzed for the level of anti-CTB IgG antibodies by antigen-capture and GM1-capture ELISA. (**B**) Characterization of three hybridomas, 7A12, 8F8 and 9F9, which showed high anti-CTB antibody levels by ELISA. The hybridoma cell culture supernatants showed distinctive binding patterns to CTB in antigen-capture vs. GM1-capture ELISA. All three hybridoma showed similarly high binding in CTB-capture ELISA. By contrast, 7A12 showed the least and negligible binding while 9F9 showed the highest binding in GM1-capture ELISA. Bars represent means ± range of technical duplicate values.

isolate single clones, and the resultant 7A12B3 and 9F9C7 hybridomas were selected for subsequent studies. The Pro-Detect™ Rapid Antibody Isotyping Kit- Rat revealed that both 7A12B3 and 9F9C7 mAbs are of the IgG2a isotype with kappa light chains.

The mAbs 7A12B3 and 9F9C7 bind CTX, CTB, and EPICERTIN with high affinities. To determine the antigen-binding properties of 7A12B3 and 9F9C7 mAbs, we initially performed antigen-capture ELISA wherein CTB, CTX, and LTB were coated on the plates. Both 7A12B3 and 9F9C7 mAbs showed similar high binding affinities to CTB, expressed as half-maximal effective concentrations (EC_{50}) of 0.028 ± 0.003 and 0.036 ± 0.003 µg/mL, respectively (Fig. 2, left panel). Likewise, 7A12B3 and 9F9C7 mAbs bound to CTX with high binding affinities represented by low EC_{50} values (0.017 ± 0.003 and 0.041 ± 0.005 µg/mL, respectively). The 9F9C7 mAb showed slightly lower affinity to CTX than 7A12B3, possibly due to marginal occlusion of the epitope by the holotoxin A subunit (Fig. 2, middle panel). Despite LTB's high amino acid sequence similarity to CTB[33,34], both 7A12B3 and 9F9C7 mAbs showed a substantially lower affinity to LTB than to CTB and CTX, with an EC_{50} value of 1.109 ± 0.162 and 135 ± 70 µg/mL, respectively (Fig. 2, right panel). Average EC_{50} values of 7A12B3 and 9F9C7 mAbs binding to all three molecules are presented in Table 1.

To further dissect the antigen-binding profiles of 7A12B3 and 9F9C7, SPR analysis was employed, in which each mAbs was immobilized on a CM5 sensor chip while CTX, CTB, EPICERTIN, and LTB were used as soluble analytes. Figure 3 shows representative sensorgrams. Analysis of binding kinetics revealed that 7A12B3 mAb had an average association rate constant (k_{on}) of 1.4×10^6 (1/Ms), a dissociation rate constant (k_{off}) of 1.8×10^{-4} (1/s), and an average equilibrium dissociation constant (K_D) of 129 pM to CTX. This mAb also showed similar high binding affinity to CTB and EPICERTIN, with average K_D values of 88.9 and 159 pM, respectively (Fig. 3A). On the other hand, 9F9C7 mAb showed slower association and slower dissociation for CTX and CTB compared to 7A12B3. The 9F9C7 mAb also showed slower association but similar dissociation to EPICERTIN, compared to 7A12B3 (Fig. 3B). Thus, 9F9C7 mAbs turned out to have overall lower binding affinities to the three analytes, as 9F9C7 showed an average K_D of 6.1 nM to CTX, 4.4 nM to CTB, and 33.2 nM to EPICERTIN. These values correspond to approximately 50 times (CTX and CTB) and 200 times (EPICERTIN) lower affinity when compared to 7A12B3. In sharp contrast, neither mAbs showed measurable binding to LTB under the conditions used in this SPR analysis (Fig. 3A,B). Average association and dissociation rate constants and K_D values are summarized in Table 2.

The 7A12B3 mAb, but not 9F9C7, blocks CTB binding to its receptor GM1. A GM1-capture ELISA was initially conducted to analyze the impact of 7A12B3 and 9F9C7 mAbs on the receptor binding activity of CTB. Consistent with our observations from the culture supernatants of the parental hybridoma clones

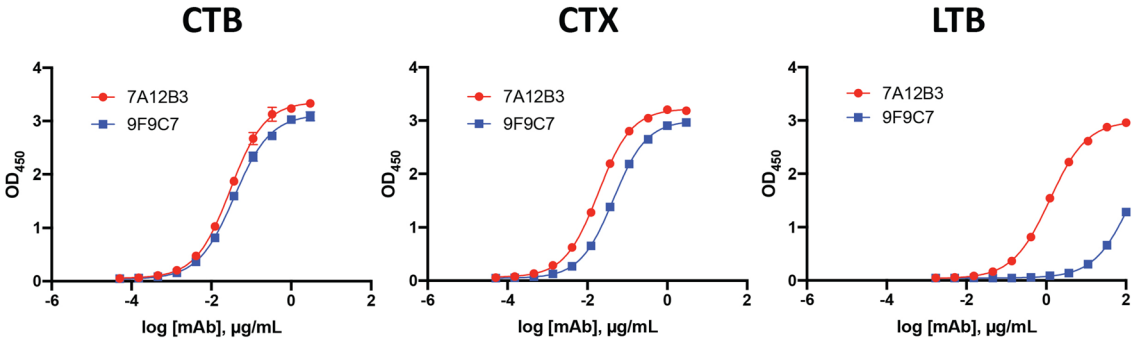

Figure 2. Analysis of 7A12B3 and 9F9C7 mAbs binding to CTX, CTB and LTB in antigen-capture ELISA. ELISA plates were coated with 2 µg/mL of CTB, CTX or the *Escherichia coli* heat-labile enterotoxin B subunit (LTB). Three-fold serially diluted 7A12B3 or 9F9C7 mAbs (3000—0.051 ng/mL for CTB and CTX; 100,000—1.69 ng/mL for LTB) were added to the plates and incubated, and plate-bound mAbs were detected with an anti-rat IgG secondary antibody. Representative graphs are shown. The assays were performed in triplicate, and each data point represents the mean ± SD. Data were analyzed and plotted using the GraphPad Prism 9 software and obtained from at least two independent experiments. The half-maximal effective concentrations (EC_{50}s) were determined by nonlinear regression analysis (GraphPad Prism 9) and displayed in Table 1.

	CTX	CTB	LTB
EC50 (µg/mL)			
7A12B3 mAb	0.017 ± 0.003	0.028 ± 0.003	1.09 ± 0.162
9F9C7 mAb	0.041 ± 0.005	0.036 ± 0.003	> 100

Table 1. Average EC_{50} values and standard deviation (N = 2) of 7A12B3 and 9F9C7 mAbs binding to CTX, CTB and LTB.

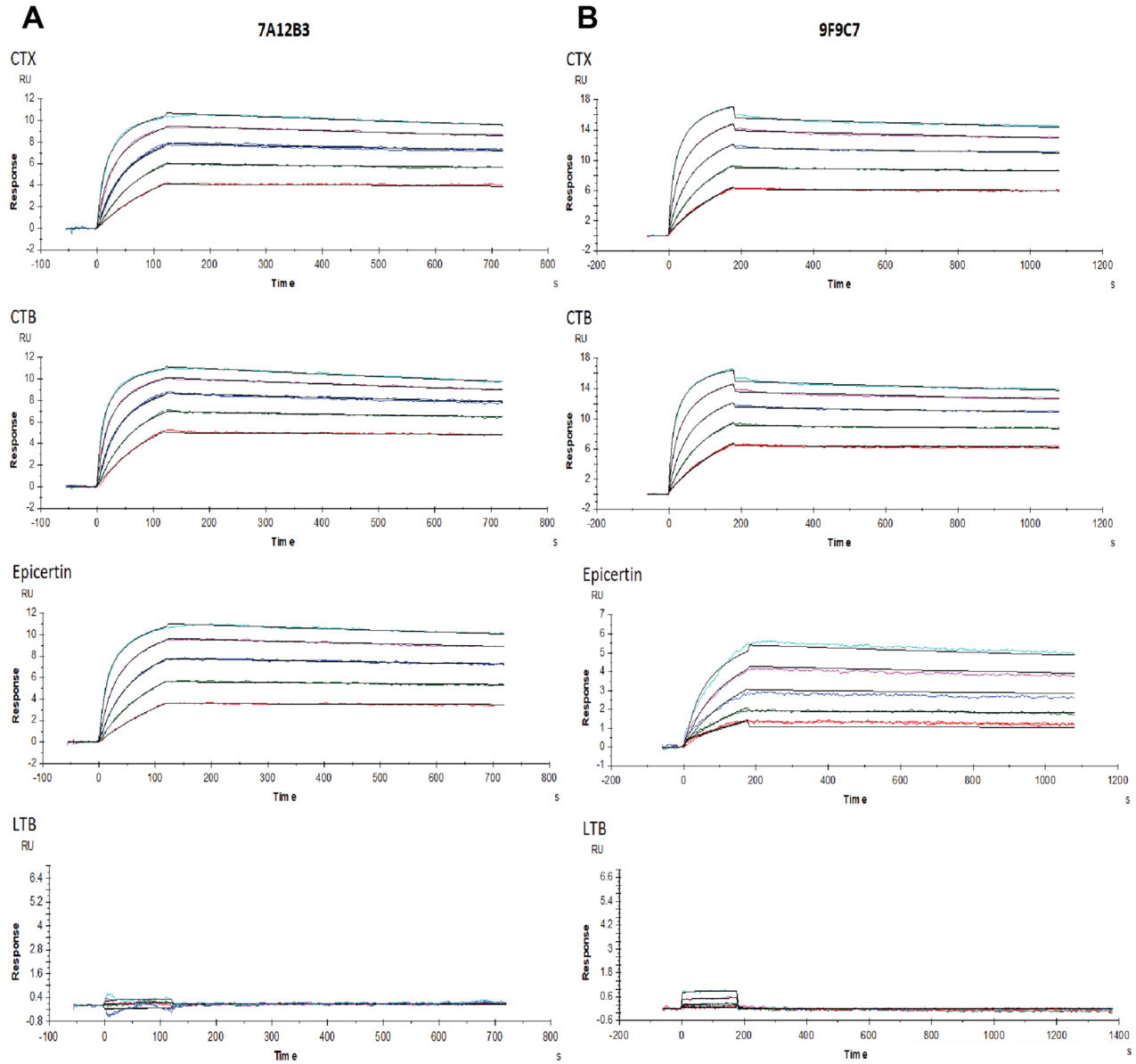

Figure 3. SPR analysis of 7A12B3 and 9F9C7 mAbs binding affinities to CTX, CTB, EPICERTIN and LTB. Each mAb was immobilized on a CM5 sensor chip. Each analyte (CTX, CTB, EPICERTIN, and LTB) was tested in a range of concentrations (0, 1.68, 3.37, 6.73, 13.47, 26.9375 nM) against immobilized 7A12B3 mAb or 9F9C7 mAb (0, 106.3, 212.5, 425, 850, 1670 nM). The collected kinetic data were blank subtracted, so the concentration at 0 nM is not shown. Representative sensorgrams for (A) 7A12B3 and (B) 9F9C7 are shown after Bivalent model fitting. Each experiment was conducted with at least three replicates.

	k_{on} (1/Ms)	k_{off} (1/s)	K_D (pM)	Chi^2 (RU^2)
7A12B3 mAb				
CTX	1.4×10^6 (1.3×10^6–1.4×10^6)	1.8×10^{-4} (1.5×10^{-4}–2.1×10^{-4})	129.0 (120.0–151.0)	7.6×10^{-3} (5.8×10^{-3}–8.8×10^{-3})
CTB	2.6×10^6 (2.4×10^6–2.8×10^6)	2.3×10^{-4} (2.0×10^{-4}–2.6×10^{-4})	88.9 (81.1–103.0)	10.0×10^{-3} (7.2×10^{-3}–16.0×10^{-3})
EPICERTIN	1.1×10^6 (1.0×10^6–1.2×10^6)	1.7×10^{-4} (1.6×10^{-4}–1.7×10^{-4})	159.0 (145.0–173.0)	6.0×10^{-3} (4.1×10^{-3}–8.0×10^{-3})
	k_{on} (1/Ms)	k_{off} (1/s)	K_D (nM)	Chi^2(RU^2)
9F9C7 mAb				
CTX	1.5×10^4 (1.4×10^4–1.5×10^4)	9.0×10^{-5} (8.4×10^{-5}–10.0×10^{-5})	6.1 (5.6–6.5)	8.3×10^{-3} (7.3×10^{-3}–9.3×10^{-3})
CTB	2.2×10^4 (2.1×10^4–2.3×10^4)	9.9×10^{-5} (1.0×10^{-4}–10.0×10^{-5})	4.4 (4.3–4.5)	9.6×10^{-3} (7.2×10^{-3}–10.6×10^{-3})
EPICERTIN	4.9×10^3 (4.8×10^3–5.0×10^3)	1.6×10^{-4} (1.4×10^{-4}–1.9×10^{-4})	33.2 (28.0–39.0)	3.0×10^{-2} (2.8×10^{-2}–3.1×10^{-2})

Table 2. Association and dissociation constants of CTX, CTB and EPICERTIN binding to 7A12B3 and 9F9C7 mAbs generated by surface plasmon resonance.

(Fig. 1B), the 7A12B3 mAb markedly blocked the binding of CTB to GM1 whereas no significant effect was observed in the presence of 9F9C7 mAb (data not shown). To analyze more rigorously the blocking properties of 7A12B3 mAb in CTB-GM1 interaction, we used a competitive GM1/KDEL ELISA, in which EPICERTIN bound to the glycosphingolipid receptor was detected using anti-KDEL mAb[22]. The 7A12B3 mAb at 0.1–1 µg/mL dose-dependently inhibited the binding of EPICERTIN to GM1 (Fig. 4A, left panel). In contrast, 9F9C7 mAb showed a relatively smaller effect on EPICERTIN binding to GM1 and only at a concentration of 1 µg/mL shifted the EPICERTIN binding curve to a level very similar to that observed with 0.1 µg/mL of 7A12B3 mAb (Fig. 4A, right panel). In a competitive GM1/KDEL ELISA in which varying concentrations of respective mAbs were pre-incubated with a fixed concentration of EPICERTIN at 100 ng/mL, the IC_{50} values for 7A12B3 and 9F9C7 mAbs on the EPICERTIN binding to GM1 were determined to be 201.2 vs. 993.7 ng/mL respectively (Fig. 4B).

The 7A12B3 mAb effectively inhibits CTX-induced cAMP in Caco2 cells. The inhibitory effects of 7A12B3 and 9F9C7 mAbs on the biological functions of CTX were analyzed in the Caco2 cell line model of cAMP induced by CTX. Figure 5A shows that CTX (0.5 µg/mL) preincubated with 7A12B3 mAb (1 µg/mL) induced a significantly lower level of cytoplasmic cAMP in Caco2 cells when compared to CTX alone (86.7% inhibition; $p < 0.0001$), whereas 9F9C7 mAb showed significant yet less inhibitory effect (62.6% inhibition; $p = 0.0032$). The inhibitory effect of 7A12B3 mAbs was significantly different from that of 9F9C7 mAb

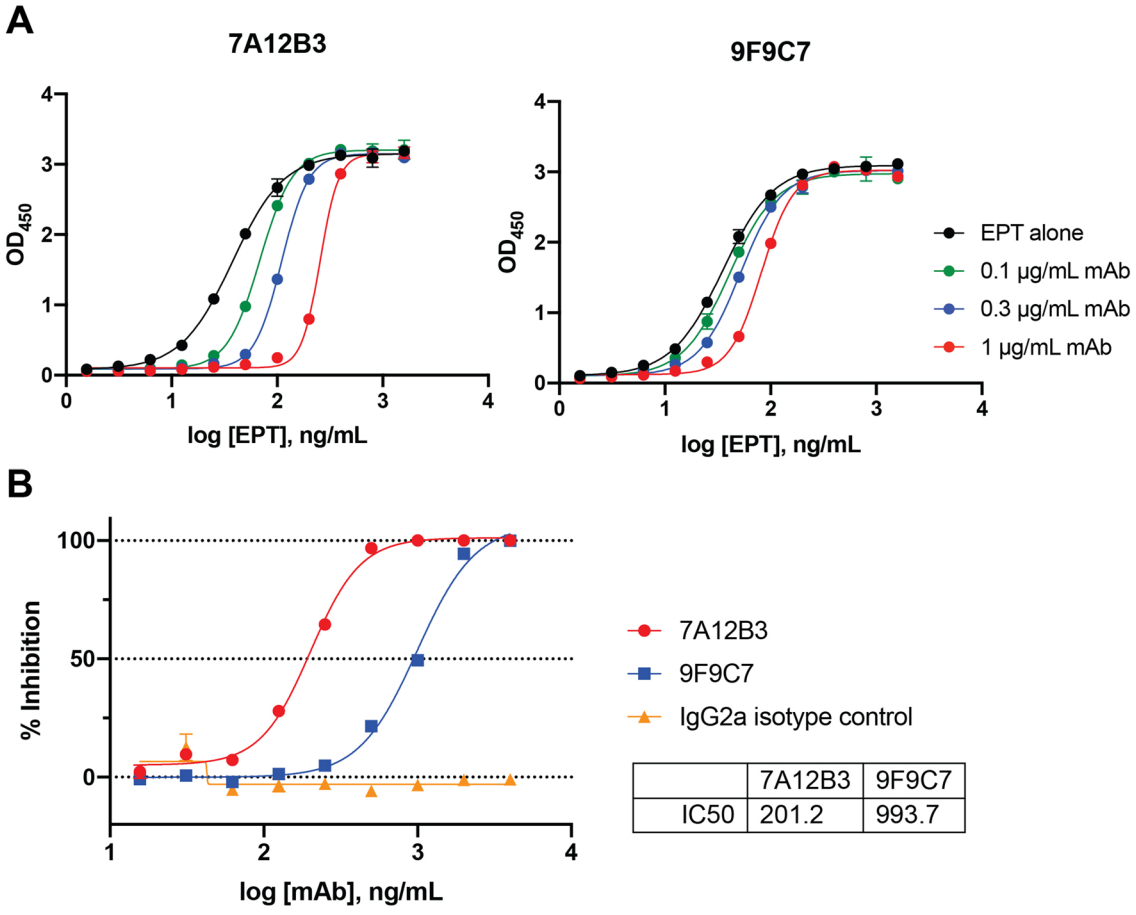

Figure 4. The 7A12B3 mAb, but not 9F9C7, blocks EPICERTIN binding to GM1 ganglioside. EPICERTIN and GM1-capture KDEL-detection (GM1/KDEL) ELISA methods were employed to reveal the impact of 7A12B3 and 9F9C7 mAbs on CTB's binding to the ganglioside receptor. (**A**) Three concentrations of each antibody (0.1, 0.3 and 1.0 µg/mL) were preincubated with varying concentrations of EPICERTIN and applied to ELISA plates coated with GM1. Plate bound EPICERTIN was detected with an anti-KDEL mAb, as described previously[22]. The 7A12B3 mAb concentration-dependently blocked the interaction of EPICERTIN with GM1 at 0.1–1 µg/mL, whereas the 9F9C7 mAb had much less effects. (**B**) A competitive GM1/KDEL ELISA was employed to determine the effect of mAbs on EPICERTIN–GM1 interaction. Varying concentrations of respective mAbs, including a rat IgG2a isotype control, were pre-incubated with 100 ng/mL of EPICERTIN and applied to ELISA plates coated with GM1. Plate-bound EPICERTIN was detected with an anti-KDEL mAb, as described previously[22]. Half maximal inhibitory concentration (IC50) of 7A12B3 (201.2 ng/mL) and 9F9C7 (993.7 ng/mL) mAbs were determined by a non-linear regression analysis using GraphPad Prism 9. Data were obtained from at least three independent experiments, and representative graph from one experiment is shown. Each data point represents the mean ± range of duplicate samples.

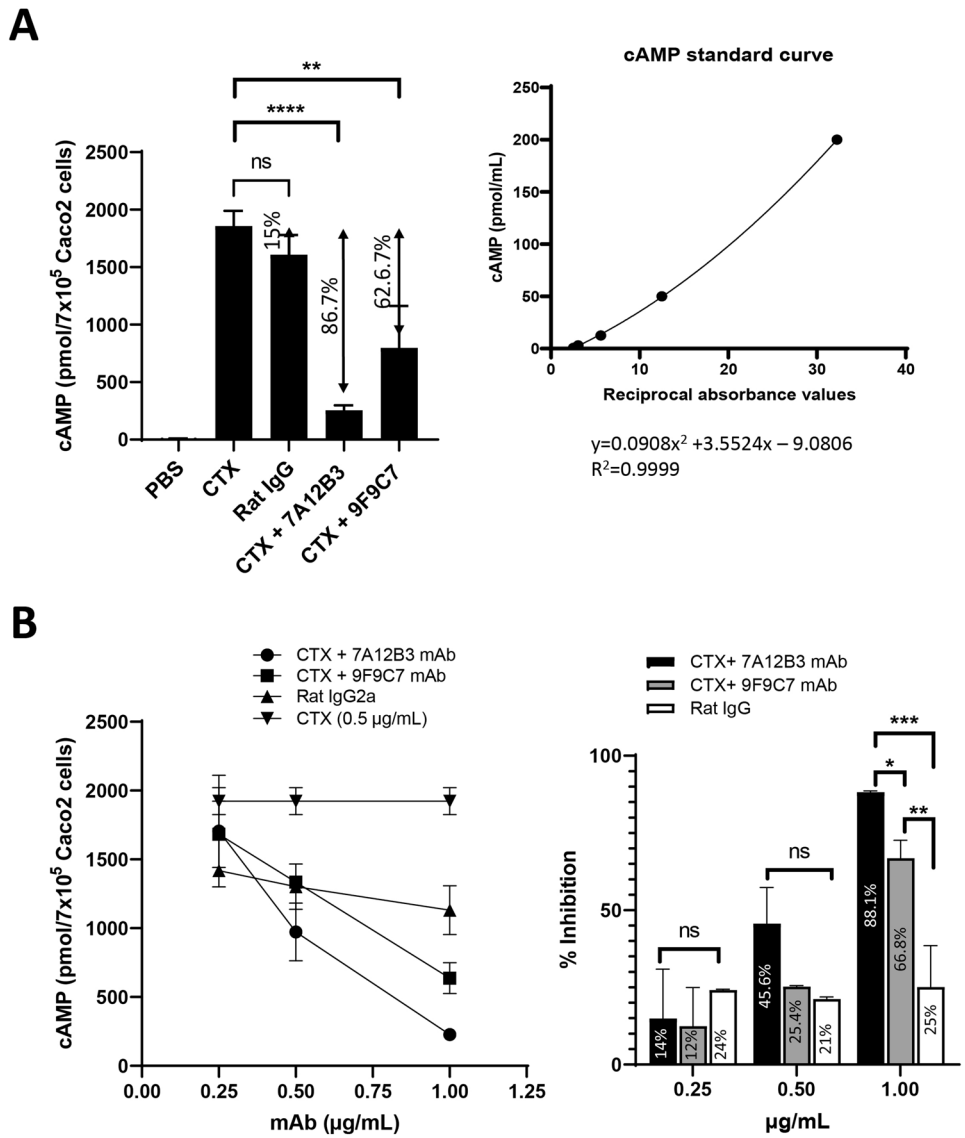

Figure 5. The 7A12B3 mAb effectively inhibits CTX-induced cAMP levels in Caco2 cells. (**A**) The inhibitory effects of 7A12B3 and 9F9C7 mAbs (0.25- 1.0 µg/mL) on CTX-induced cAMP were evaluated under preincubation of the mAbs with CTX (0.5 µg/mL) for 20 min. The 7A12B3 mAb (1.0 µg/mL) strongly inhibited CTX-induced cAMP levels in Caco2 cells, whereas 9F9C7 at the same concentration had reduced inhibitory effects. $^{****}p < 0.0001$, $^{**}p < 0.01$, one-way measures ANOVA with Bonferroni's multiple comparisons tests. Inset shows a standard curve of cAMP, with a non-linear regression analysis (GraphPad Prism 9) used to determine cAMP values in samples. (**B**) Concentration-dependent inhibition of CTX (0.5 µg/mL)-induced cAMP levels in Caco2 cells by 7A12B3 and 9F9C9 mAbs. $^{*}p < 0.05$, $^{**}p < 0.01$, two-way measures ANOVA with Bonferroni's multiple comparisons tests. Data obtained from two independent experiments. Each data point represents the mean ± SD of triplicate samples.

($p = 0.0274$) or a rat IgG2a isotype control ($p = 0.0002$). The marginal inhibition observed with a rat IgG2a isotype control antibody was not statistically significant from the PBS vehicle control ($p = 0.0626$). The inhibitory effects of 7A12B3 and 9F9C7 mAbs on CTX-induced elevation of cAMP in Caco2 cells were concentration dependent (Fig. 5B). When CTX was co-incubated with 1 µg/mL of mAbs, 7A12B3 inhibited the induction of cAMP by 88.1%, whereas significantly less inhibition was observed with 9F9C7 mAb (66.8%). Both mAbs had minimal inhibitory effects at 0.25 µg/mL (14% vs. 12%, respectively), which were indistinguishable from the background effects of a Rat IgG isotype control antibody.

The 9F9C7 mAb effectively detects CTB docking on the surface of target cells. Flow cytometric analysis was conducted to evaluate the utility of 7A12B3 and 9F9C7 mAbs to detect CTB and its variants bound to the surface of target cells. Although 7A12B3 was able to detect EPICERTIN on the surface of Caco2 epithelial

cells, 9F9C7 showed superior detectability with increased fluorescence signal at the same concentration used (Fig. 6A, left panel). Thus, the latter mAb was used in further analysis.

Using the 9F9C7 mAb, we observed strong and comparable binding of EPICERTIN and CTB to the surface of Caco2 cells, similar to our previous findings[23]. However, here we found that EPICERTIN^{G33D}, a variant lacking GM1-binding activity, was only marginally detected on the cell surface, while the whole population of Caco2 cells bound CTB and EPT (Fig. 6A, right panel). Next, we attempted to characterize EPICERTIN's target immune cells using 9F9C7 mAb. To this end, mouse spleen cells were incubated with EPICERTIN or EPICERTIN^{G33D}, followed by staining with different combination of cell-surface marker-specific antibodies and 9F9C7, and gated to sort target cell subpopulations, as shown in Fig. 6B. The geometric mean fluorescence intensity (G-MFI) of EPICERTIN and EPICERTIN^{G33D} detected with FITC-labeled goat anti-Rat IgG antibody above the background levels generated by this second antibody alone is shown in Fig. 6C. We found that EPICERTIN efficiently bound to the surface of all myeloid and lymphoid cells analyzed, with major histocompatibility complex class II (MHC II)-positive dendritic cells and macrophages being the most prominent targets. Surprisingly, EPICRTIN^{G33D} appeared to recognize some of the cell types, including B cells, monocytes, macrophages, and dendritic cells, although the degrees of binding to these cells were overall much lower compared to EPICERTIN (Fig. 6C).

The 9F9C7 mAb detects EPICERTIN by immunohistochemistry on frozen colon sections. Fluorescent immunohistochemistry was conducted using FITC-conjugated 9F9C7 mAb to detect and locate EPICERTIN bound to the surface of colon epithelial cells upon oral administration of the protein in mice. EPICERTIN was detected on frozen colon tissue sections at 6, 12 and 24 h after oral administration of the protein, whereas it was not detected in untreated animal tissues or 0 and 3 h after oral administration. Representative confocal images of an EPICERTIN-treated animal tissue isolated 24 h post oral administration and a tissue from a control untreated animal are shown in Fig. 7. The tissue was stained with antibodies to the epithelial cell–cell adhesion protein E-cadherin and the lectin WGA to discriminate the apical plasma membrane of colon epithelial cells and the membrane-enclosed secretory granules of goblet cells within the crypt. Of note, the fluo-

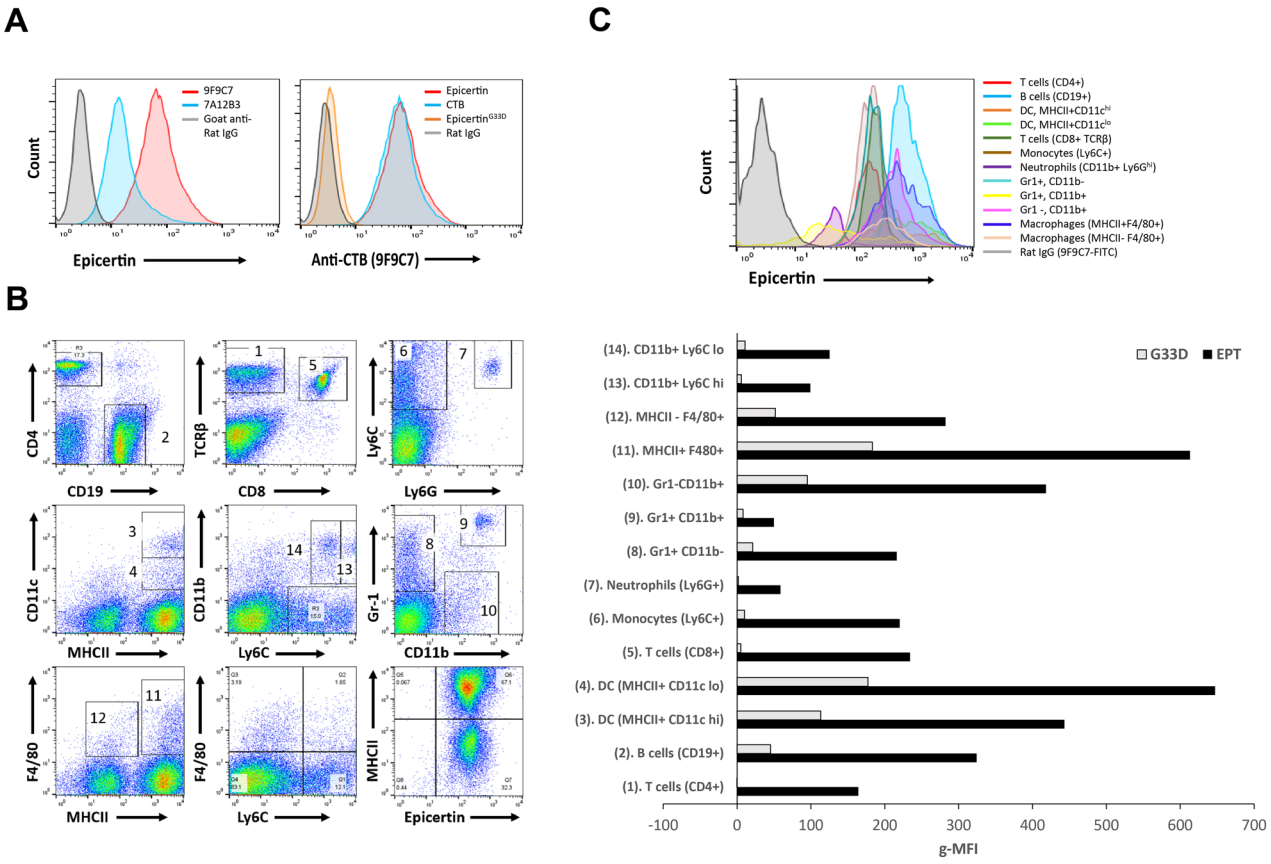

Figure 6. The 9F9C7 mAb detects EPICERTIN but not EPICERTIN^{G33D} bound to the surface of human Caco2 cell line and to mouse spleen leukocytes. (**A**) Flow cytometry analysis of EPICERTIN binding to Caco2 cells detected with 2 µg/mL of 7A12B3 or 9F9C7 mAbs followed by FITC-labeled goat-anti-rat IgG (left panel). Detection of EPICERTIN, CTB and EPICERTIN^{G33D} (2 µg/mL) binding to human Caco2 cell line detected with anti-CTB 9F9C9 mAb (right panel). (**B**) Staining pattern and gated spleen leukocytes that were screened for EPICERTIN and EPICERTIN^{G33D} binding by flow cytometry. Spleen leukocytes were incubated with 5 µg/mL of EPICERTIN or EPICERTIN^{G33D} for 30 min on ice and then stained with a panel of fluorochrome-labeled antibodies and FITC-conjugated 9F9C7 anti-CTB mAb. (**C**) Histograms and geometric mean fluorescence intensity of EPICERTIN and EPICERTIN^{G33D} bound to the mouse spleen leukocytes gated in panel B.

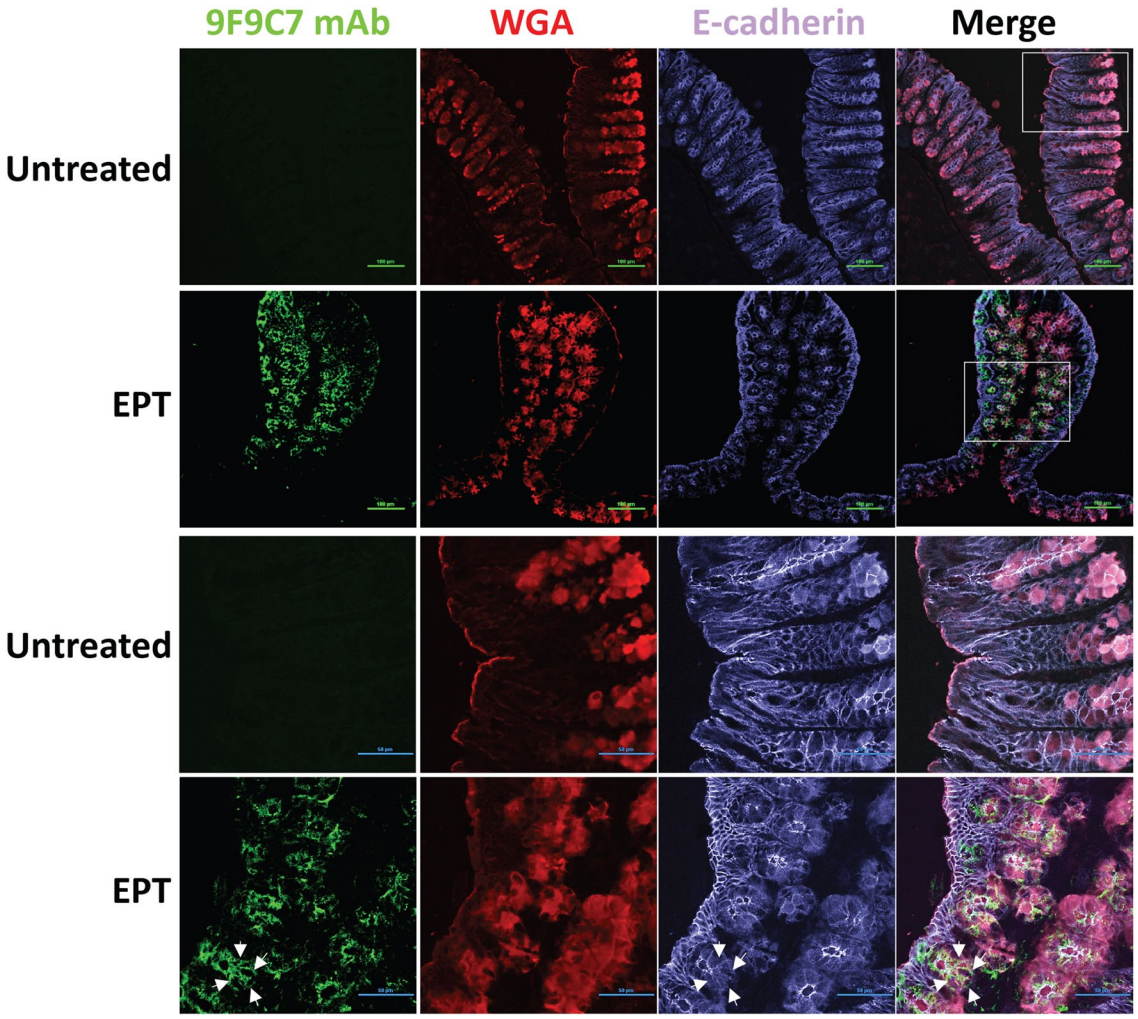

Figure 7. IHC detection of EPICERTIN bound to the surface epithelial cells of mouse colon tissue. Confocal laser scanning microcopy of colon tissues from mice treated or left untreated with EPICERTIN by oral gavage. Colon tissues were collected from EPICERTIN-dosed mice at 0, 3, 6, 12, and 24 h after oral administration or from untreated animals and embedded in OCT compound for cryosectioning. Seven microns thick tissue sections were made and stained with 5 µg/mL Pheno Vue Fluor 594-WGA, 2 µg/mL anti-E-cadherin and 2 µg/mL anti-CTB (FITC-9F9C7 mAb). Representative confocal images of an EPICERTIN-treated animal tissue isolated at 24 h and a tissue from a control untreated animal are shown. White arrows indicate distribution of EPT at the plasma membrane of individual colon crypt epithelial cells. Images were collected with a Nikon A1R Confocal laser scanning microscope using 20 × (top panel) and 60 × (lower panel) magnification lenses with appropriate channels and the data processed with the NIS Elements imaging software. Areas delineated by dotted line squares in panel A correspond to high magnification images shown in lower panel.

rescence signal was consistently detected on epithelial cells within the colonic glands while not prominent on epithelial cells facing the luminal side of the colon (Fig. 7). The staining of EPICERTIN delineated the luminal side of differentiated crypt epithelial cells (near the colon crypt opening) and less differentiated epithelial cells located at the bottom of the crypts. Additionally, the image disclosed that EPICERTIN's fluorescence signal at the plasma membrane seem to follow closely that of the adhesion molecule E-cadherin (although not overlapping) in less differentiated and mucin-rich crypt epithelial cells. Meanwhile, FITC-9F9C7 mAb did not show any fluorescence signal in colon tissues from EPICERTIN-untreated mice, confirming the specificity of the antibody.

Discussion

Since the introduction of hybridoma technology over 45 years ago[30], several anti-CTX mAbs targeting different epitopes on the A and B subunits have been generated in early studies[35–40]. Some of those mAbs recognized the GM1 receptor binding site of CTB or showed distinctive neutralizing CTX activity[41], whereas other mAbs that were generated against CTX peptides, often resulted in the generation of mAbs with polyspecific binding properties or completely lacked CTX binding activity[42,43]. They aided in building the current understanding of CTX secretion, assembly[44,45], endocytosis and intoxication[46], and were also instrumental in understanding the potent immunogenicity of CTB and the structurally homologous LTB[36,47]. However, most of those anti-CTB

mAbs were characterized only using outdated immunoassay-based methods, providing limited information about their binding profiles. Recently, novel recombinant CTB variants and fusion molecules have been generated, some of which were found to have unique biological functions, such as mucosal healing promoted by a CTB variant containing an ER retention motif, EPICERTIN[21,23]. To aid in the preclinical development of CTB-based vaccines and biotherapeutics, we attempted to isolate and characterize new anti-CTB mAbs that are suitable for mechanistic investigations and pharmacological studies.

The 7A12 and 9F9 hybridoma cell culture supernatants were found to bind CTB with distinctive features in both antigen- and GM1-capture ELISAs (Fig. 1). Both mAbs bound CTB with high affinity, but only 9F9 effectively bound CTB in GM1-capture ELISA, indicating that 7A12 recognizes an epitope near or within the region of CTB responsible for GM1 interaction. On the other hand, the 9F9 hybridoma supernatant appeared to recognize a distinct epitope most probably not involved in GM1 binding. These results demonstrate that our screening procedure employed here successfully led to the isolation of two mAbs with distinct CTB-binding profiles in terms of reactivity with the antigen's GM1-receptor binding site.

The 7A12B3 and 9F9C7 mAbs were found to bind the native CTX and CTB with similar binding affinities in direct ELISA (Fig. 2, Table 1). However, SPR analysis revealed that these mAbs have distinct binding kinetics. The overall binding affinity of 7A12B3 mAb was higher than that of 9F9C7 mAb; 159 pM vs. 33.2 nM for EPICERTIN, 129 pM vs. 6.1 nM for CTX, and 88.9 pM vs. 4.4 nM for CTB, respectively (Fig. 3, Table 2). In contrast, neither 7A12B3 or 9F9C7 bound to LTB in SPR (Fig. 3), along the lines of the ELISA data that also showed substantially low affinity of these mAbs to LTB compared to CTB and CTX (Fig. 2). These results demonstrate the exquisite specificity of 7A12B3 and 9F9C7 mAbs to CTB, given that LTB has high (~ 84%) amino-acid sequence homology with CTB[33,34]. The binding affinity of 7A12B3 to EPICERTIN was slightly lower than to CTX or CTB, and those differences might be explained by the Asn4 → Ser mutation and/or the presence of C-terminal extension comprised of the hexapeptide SEKDEL sequence in EPICERTIN. Of note, 7A12B3 mAb but not 9F9C7 effectively inhibited the binding of EPICERTIN to GM1 ganglioside (Fig. 4), strengthening the idea that the former recognizes an epitope near the GM1 binding site of CTB, whereas the latter is relatively indifferent to CTB-GM1 interaction.

CTX induces cAMP overproduction in the cytoplasm of target cells. Our data demonstrated that the 7A12B3 mAb has strong CTX-neutralizing effects, almost completely inhibiting the cytoplasmic accumulation of cAMP induced by CTX in Caco2 cells (Fig. 5B). Interestingly, even though 9F9C7 mAb appeared to bind to an epitope distal to the GM1-binding site, we found that the mAb was also able to inhibit the effects of CTX on the elevation of cytoplasmic cAMP in Caco2 cells, although at lower levels than 7A12B3 mAb. We speculate that 9F9C7 mAb may form complexes with CTX in solution, which in turn collaterally compromises CTX-GM1 interaction and/or entry to target cells.

Based on the results from the competitive ELISA (Fig. 4) and CTX cAMP reporter assays (Fig. 5), 7A12B3 was thought to target an epitope proximal to the GM1 binding site, an area of CTB that would be occluded after engaging the cell-surface glycosphingolipid receptor. However, flow cytometry analysis revealed that the mAb is capable of detecting EPICERTIN on the surface of Caco2 epithelial cells (Fig. 6A, left panel). Nevertheless, 9F9C7, which was selected based on effective recognition of GM1-bound CTB (Fig. 1B), showed superior detectability of cell-bound EPICERTIN and thus justified the use of this mAb to explore the target cell binding profile of EPICERTIN. The flow cytometry analysis (Fig. 6) revealed that EPICERTIN and CTB equally bound to the surface of Caco2 cells, as anticipated from their similar binding affinity to GM1 ganglioside[19]. In sharp contrast, EPICERTIN^{G33D} was only marginally detected on the cell surface (Fig. 6A, right panel), suggesting that the glycosphingolipid is the primary receptor for EPICERTIN in the colon epithelial cell line. To our surprise, however, we found inconsistent binding patterns of EPICERTIN and EPICERTIN^{G33D} in mouse spleen leukocytes. For instance, EPICERTIN's geometric mean fluorescence intensity (gMFI) ranged between 50 and 300 whereas the gMFI of EPICERTIN^{G33D} ranged from 0 to 45 (Fig. 6B,C). Although GM1 ganglioside has been long considered the sole receptor for CTB binding and internalization by epithelial cells, recent findings pointed to the presence of alternative receptors, such as fucosylated glycoconjugates[48–50]. In addition, cycling of KDEL receptors between the Golgi and cell membrane[51] could partly account for the cellular binding patterns of EPICERTIN and the G33D variant. Thus, differential expression of those receptors might explain CTB binding to leukocytes in a cell type specific manner. Nevertheless, because the degree of binding was overall substantially higher with EPICERTIN than with the non-GM1-binding counterpart, it seems reasonable to assume that EPICERTIN's effects on immune cells are likely mediated by GM1 receptor engagement.

The expression of GM1 is not limited to intestinal epithelial cells. It is expressed in a variety of other cell types, including cortical and peripheral neurons[52,53] and leukocytes[50], among others. A differential expression of GM1 on human monocytes suggested the presence of two monocytes subpopulations with functional differences in terms of endocytic activity and lipopolysaccharide responsiveness in peripheral blood[54]. CTB is known to bind to GM1 expressed on the surface of leukocytes, particularly innate immune cells such as dendritic cells, macrophages and B cells, which are the major antigen-presenting cells[8]. CTB binding to GM1 on B cells was associated with cAMP-independent inhibition of mitogen-stimulated B cell proliferation and enhanced expression of MHCII molecules[26,55], whereas binding of CTB on T lymphocytes was found to inhibit mitogen or antigen-induced T-cell proliferation[26]. Of note, however, the nature of the enhanced immune responses to antigens coupled to CTB and the dampening of autoimmune responses by this protein are still largely unknown. In the case of antibody-mediated immune responses against infectious microorganisms, the increased MHC II expression on B cells induced by CTB might partially explain the immunomodulatory effect favoring this outcome[8]. In the case of suppression of airway allergic inflammation, CTB's therapeutic effect appeared to reside in its capacity to reprogram dendritic cells to instruct B cells for IgA class switch[56]. As shown in Fig. 6, EPICERTIN highly bound to antigen-presenting cells compared to other leukocytes, particularly MHC II$^+$ CD11c^{lo} dendritic cells, MHC II$^+$ F480$^+$ macrophages and CD19$^+$ B cells. Although it remains a matter of speculation at this point, such

preferential binding may suggest EPICERTIN's distinctive effects on these cells that could have implications for the protein's immunomodulatory effects.

The specific interaction of CTB with GM1 ganglioside expressed on the surface of intestinal epithelial cells is a well-known mechanism responsible for the internalization of CTX and its virulence during *V. cholerae* infection[57]. This high affinity interaction has been exploited in vaccine development where CTB is used as an adjuvant and carrier protein. Additionally, the ability of CTB to undergo retrograde transportation in target cells may provide opportunities for the development of novel pharmaceutical products with unique biological functions, as exemplified by EPICERTIN, which was found to be retained in the ER of colon epithelial cells where it induces an unfolded protein response leading to epithelial repair activity[21]. However, the type of colon epithelial cell targeted/responsible for such a response remains to be identified. In the IHC analysis on cryosections of mouse colon tissue using the 9F9C7 mAb (Fig. 7), we were able to clearly detect EPICERTIN in the colon at 6 h and up to 24 h after oral administration. Interestingly, EPICERTIN was detected mainly on the surface of epithelial cells lining the openings of colonic crypts with consistent detection on less differentiated cells at the bottom of the crypts, including crypt-resident goblet cells that are densely stained with the WGA lectin[58]. This observation suggests that EPICERTIN might have prominent effects on the colon stem cell compartment with proliferative capability than on differentiated epithelial cells. However, this conjecture needs further verification as we cannot rule out the possibility that the detection of EPICERTIN mostly in the crypt base region might be a procedural artifact during the flushing procedure of colons before tissue embedding, which could have inadvertently removed EPICERTIN bound to the inter-crypt epithelium exposed on the luminal side. Our future study will address this issue by further IHC analysis of ex vivo-cultured mouse and human colon tissues.

In conclusion, the present study demonstrated that mAbs 7A12B3 and 9F9C7 bind CTX, CTB and EPICERTIN with high affinity and specificity. The 7A12B3 mAb effectively inhibited the binding of CTB to GM1 and neutralized CTX, whereas the 9F9C7 mAb showed superior capacity to detect EPICERTIN binding to the surface of target cells. Coupled with our earlier reports showing the utility of 9F9C7 in immunofluorescence and immunoprecipitation[23] and 7A12B3 in rodent pharmacokinetic analysis of EPICERTIN[25], these mAbs provide valuable tools to facilitate the investigation and development of CTB variants as novel biopharmaceutical candidates.

Data availability

The datasets generated during the current study are available from the corresponding author on reasonable request.

Received: 26 October 2022; Accepted: 2 March 2023
Published online: 15 March 2023

References

1. Harris, J., LaRocque, R., Qadri, F., Ryan, E. & Calderwood, S. Cholera. *Lancet* **379**, 2466–2476 (2012).
2. Cuatrecasas, P. Interaction of *Vibrio cholerae* enterotoxin with cell membranes. *Biochemistry* **12**, 3547–3558 (1973).
3. Holmgren, J., Lönnroth, I. & Svennerholm, L. Fixation and inactivation of cholera toxin by GM1 ganglioside. *Scand. J. Infect. Dis.* **5**, 77–78 (1973).
4. Merritt, E. A. *et al.* Crystal structure of cholera toxin B-pentamer bound to receptor GM1 pentasaccharide. *Protein Sci.* **3**, 166–175 (1994).
5. Holmgren, J., Czerkinsky, C., Lycke, N. & Svennerholm, A.-M. Strategies for the induction of immune responses at mucosal surfaces making use of cholera toxin B subunit as immunogen, carrier, and adjuvant. *Am. J. Trop. Med. Hyg.* **50**, 42–54 (1994).
6. Azegami, T., Itoh, H., Kiyono, H. & Yuki, Y. Novel transgenic rice-based vaccines. *Arch. Immunol. Ther. Exp.* **63**, 87–99 (2015).
7. Baldauf, K. J., Royal, J. M., Hamorsky, K. T. & Matoba, N. Cholera toxin B: one subunit with many pharmaceutical applications. *Toxins* **7**, 974–996 (2015).
8. Stratmann, T. Cholera toxin subunit B as adjuvant—An accelerator in protective immunity and a break in autoimmunity. *Vaccines* **3**, 579–596 (2015).
9. Solbreux, P. M., Dive, C. & Vaerman, J.-P. Anti-cholera toxin IgA-, IgG-and IgM-secreting cells in various rat lymphoid tissues after repeated intestinal or parenteral immunizations. *Immunol. Invest.* **19**, 435–451 (1990).
10. Apter, F., Lencer, W., Finkelstein, R., Mekalanos, J. & Neutra, M. Monoclonal immunoglobulin A antibodies directed against cholera toxin prevent the toxin-induced chloride secretory response and block toxin binding to intestinal epithelial cells in vitro. *Infect. Immun.* **61**, 5271–5278 (1993).
11. Sanchez, J., Johansson, S., Löwenadler, B., Svennerholm, A. & Holmgren, J. Recombinant cholera toxin B subunit and gene fusion proteins for oral vaccination. *Res. Microbiol.* **141**, 971–979 (1990).
12. Vendetti, S. *et al.* Polyclonal Treg cells enhance the activity of a mucosal adjuvant. *Immunol. Cell Biol.* **88**, 698–706 (2010).
13. Arakawa, T. *et al.* A plant-based cholera toxin B subunit–insulin fusion protein protects against the development of autoimmune diabetes. *Nat. Biotechnol.* **16**, 934–938 (1998).
14. Tarkowski, A., Sun, J. B., Holmdahl, R., Holmgren, J. & Czerkinsky, C. Treatment of experimental autoimmune arthritis by nasal administration of a type II collagen–cholera toxoid conjugate vaccine. *Arthritis Rheum.* **42**, 1628–1634 (1999).
15. Rask, C. *et al.* Prolonged oral treatment with low doses of allergen conjugated to cholera toxin B subunit suppresses immunoglobulin E antibody responses in sensitized mice. *Clin. Exp. Allergy* **30**, 1024–1032 (2000).
16. Phipps, P. A. *et al.* Prevention of mucosally induced uveitis with a HSP60-derived peptide linked to cholera toxin B subunit. *Eur. J. Immunol.* **33**, 224–232 (2003).
17. Ruhlman, T., Ahangari, R., Devine, A., Samsam, M. & Daniell, H. Expression of cholera toxin B–proinsulin fusion protein in lettuce and tobacco chloroplasts—Oral administration protects against development of insulitis in non-obese diabetic mice. *Plant Biotechnol. J.* **5**, 495–510 (2007).
18. Sun, J. B., Czerkinsky, C. & Holmgren, J. Mucosally induced immunological tolerance, regulatory T cells and the adjuvant effect by cholera toxin B subunit. *Scand. J. Immunol.* **71**, 1–11 (2010).
19. Hamorsky, K. T. *et al.* Rapid and scalable plant-based production of a cholera toxin B subunit variant to aid in mass vaccination against cholera outbreaks. *PLoS Negl. Trop. Dis.* **7**, e2046. https://doi.org/10.1371/journal.pntd.0002046 (2013).
20. Reeves, M. A. *et al.* Spray-dried formulation of epicertin, a recombinant cholera toxin B subunit variant that induces mucosal healing. *Pharmaceutics* **13**, 576 (2021).

21. Baldauf, K. *et al.* Oral administration of a recombinant cholera toxin B subunit promotes mucosal healing in the colon. *Mucosal Immunol.* **10**, 887–900 (2017).
22. Morris, D. A., Reeves, M. A., Royal, J. M., Hamorsky, K. T. & Matoba, N. Isolation and detection of a KDEL-tagged recombinant cholera toxin B subunit from *Nicotiana benthamiana*. *Process Biochem.* **101**, 42–49 (2021).
23. Royal, J. M. *et al.* A modified cholera toxin B subunit containing an ER retention motif enhances colon epithelial repair via an unfolded protein response. *FASEB J.* **33**, 13527–13545 (2019).
24. Royal, J. M., Reeves, M. A. & Matoba, N. Repeated oral administration of a KDEL-tagged recombinant cholera toxin B subunit effectively mitigates DSS colitis despite a robust immunogenic response. *Toxins* **11**, 678. https://doi.org/10.3390/toxins11120678 (2019).
25. Tuse, D. *et al.* Pharmacokinetics and safety studies in rodent models support development of EPICERTIN as a novel topical wound-healing biologic for ulcerative colitis. *J. Pharmacol. Exp. Ther.* **380**, 162–170 (2022).
26. Woogen, S. D., Ealding, W. & Elson, C. O. Inhibition of murine lymphocyte proliferation by the B subunit of cholera toxin. *J. Immunol.* **139**, 3764–3770 (1987).
27. George-Chandy, A. *et al.* Cholera toxin B subunit as a carrier molecule promotes antigen presentation and increases CD40 and CD86 expression on antigen-presenting cells. *Infect. Immun.* **69**, 5716–5725 (2001).
28. Canziani, G. A., Klakamp, S. & Myszka, D. G. Kinetic screening of antibodies from crude hybridoma samples using Biacore. *Anal. Biochem.* **325**, 301–307 (2004).
29. Matoba, N., Davis, K. R. & Palmer, K. E. Recombinant protein expression in *Nicotiana*. *Methods Mol. Biol.* **701**, 199–219 (2011).
30. Kohler, G. & Milstein, C. Continuous cultures of fused cells secreting antibody of predefined specificity. *Nature* **256**, 495–497 (1975).
31. Tabll, A., Abbas, A. T., El-Kafrawy, S. & Wahid, A. Monoclonal antibodies: Principles and applications of immmunodiagnosis and immunotherapy for hepatitis C virus. *World. J. Hepatol.* **7**, 2369–2383 (2015).
32. Yu, R. K., Usuki, S., Itokazu, Y. & Wu, H. C. Novel GM1 ganglioside-like peptide mimics prevent the association of cholera toxin to human intestinal epithelial cells in vitro. *Glycobiology* **26**, 63–73 (2016).
33. Holmner, A., Askarieh, G., Okvist, M. & Krengel, U. Blood group antigen recognition by *Escherichia coli* heat-labile enterotoxin. *J. Mol. Biol.* **371**, 754–764 (2007).
34. Lebens, M. *et al.* Synthesis of hybrid molecules between heat-labile enterotoxin and cholera toxin B subunits: Potential for use in a broad-spectrum vaccine. *Infect. Immun.* **64**, 2144–2150 (1996).
35. Jobling, M. G. & Holmes, R. K. Mutational analysis of ganglioside GM1-binding ability, pentamer formation, and epitopes of cholera toxin B (CTB) subunits and CTB/heat-labile enterotoxin B subunit chimeras. *Infect. Immun.* **70**, 1260–1271 (2002).
36. Holmes, R. K. & Twiddy, E. M. Characterization of monoclonal antibodies that react with unique and cross-reacting determinants of cholera enterotoxin and its subunits. *Infect. Immun.* **42**, 914–923 (1983).
37. Robb, M., Nichols, J. C., Whoriskey, S. K. & Murphy, J. R. Isolation of hybridoma cell lines and characterization of monoclonal antibodies against cholera enterotoxin and its subunits. *Infect. Immun.* **38**, 267–272 (1982).
38. Chou, S. F. Production and purification of monoclonal and polyclonal antibodies against cholera toxin. *Hybrid. Hybridomics* **23**, 258–261 (2004).
39. Kenimer, J. G., Probst, P. G., Karpas, A. B., Burns, D. L. & Kaslow, H. R. Monoclonal antibodies against the enzymatic subunit of both pertussis and cholera toxins. *Dev. Biol. Stand.* **73**, 133–141 (1991).
40. Remmers, E. F., Colwell, R. R. & Goldsby, R. A. Production and characterization of monoclonal antibodies to cholera toxin. *Infect. Immun.* **37**, 70–76 (1982).
41. Ludwig, D. S., Holmes, R. K. & Schoolnik, G. K. Chemical and immunochemical studies on the receptor binding domain of cholera toxin B subunit. *J. Biol. Chem.* **260**, 12528–12534 (1985).
42. Otte, L., Knaute, T., Schneider-Mergener, J. & Kramer, A. Molecular basis for the binding polyspecificity of an anti-cholera toxin peptide 3 monoclonal antibody. *J. Mol. Recognit.* **19**, 49–59 (2006).
43. Anglister, J. & Zilber, B. Antibodies against a peptide of cholera toxin differing in cross-reactivity with the toxin differ in their specific interactions with the peptide as observed by 1H NMR spectroscopy. *Biochemistry* **29**, 921–928 (1990).
44. Tinker, J. K., Erbe, J. L., Hol, W. G. & Holmes, R. K. Cholera holotoxin assembly requires a hydrophobic domain at the A-B5 interface: Mutational analysis and development of an in vitro assembly system. *Infect. Immun.* **71**, 4093–4101 (2003).
45. Reichow, S. L., Korotkov, K. V., Hol, W. G. & Gonen, T. Structure of the cholera toxin secretion channel in its closed state. *Nat. Struct. Mol. Biol.* **17**, 1226–1232 (2010).
46. Torgersen, M. L., Skretting, G., van Deurs, B. & Sandvig, K. Internalization of cholera toxin by different endocytic mechanisms. *J. Cell. Sci.* **114**, 3737–3747 (2001).
47. Belisle, B. W., Twiddy, E. M. & Holmes, R. K. Monoclonal antibodies with an expanded repertoire of specificities and potent neutralizing activity for *Escherichia coli* heat-labile enterotoxin. *Infect. Immun.* **46**, 759–764 (1984).
48. Sethi, A. *et al.* Cell type and receptor identity regulate cholera toxin subunit B (CTB) internalization. *Interface Focus* **9**, 20180076. https://doi.org/10.1098/rsfs.2018.0076 (2019).
49. Wands, A. M. *et al.* Fucosylation and protein glycosylation create functional receptors for cholera toxin. *Elife* **4**, e09545. https://doi.org/10.7554/eLife.09545 (2015).
50. Cervin, J. *et al.* GM1 ganglioside-independent intoxication by Cholera toxin. *PLOS Pathog.* **14**, e1006862. https://doi.org/10.1371/journal.ppat.1006862 (2018).
51. Jia, J. *et al.* KDEL receptor is a cell surface receptor that cycles between the plasma membrane and the Golgi via clathrin-mediated transport carriers. *Cell. Mol. Life. Sci.* **78**, 1085–1100 (2021).
52. Kozireski-Chuback, D., Wu, G. & Ledeen, R. W. Developmental appearance of nuclear GM1 in neurons of the central and peripheral nervous systems. *Dev. Brain Res.* **115**, 201–208 (1999).
53. Okada, E., Maeda, T. & Watanabe, T. Immunocytochemical study on cholera toxin binding sites by monoclonal anti-cholera toxin antibody in neuronal tissue culture. *Brain Res.* **242**, 233–241 (1982).
54. Moreno-Altamirano, M. M. B., Aguilar-Carmona, I. & Sánchez-García, F. J. Expression of GM1, a marker of lipid rafts, defines two subsets of human monocytes with differential endocytic capacity and lipopolysaccharide responsiveness. *Immunology* **120**, 536–543 (2007).
55. Francis, M. *et al.* Cyclic AMP-independent effects of cholera toxin on B cell activation. II. Binding of ganglioside GM1 induces B cell activation. *J. Immunol.* **148**, 1999–2005 (1992).
56. Smits, H. *et al.* Cholera toxin B suppresses allergic inflammation through induction of secretory IgA. *Mucosal Immunol.* **2**, 331–339 (2009).
57. Holmgren, J., Lönnroth, I. & Svennerholm, L. Tissue receptor for cholera exotoxin: postulated structure from studies with GM1 ganglioside and related glycolipids. *Infect. Immun.* **8**, 208–214 (1973).
58. Nystrom, E. E. L. *et al.* An intercrypt subpopulation of goblet cells is essential for colonic mucus barrier function. *Science* **372**, eabb1590. https://doi.org/10.1126/science.abb1590 (2021).

Acknowledgements
We thank Wendy Cecil and Micaela Reeves for critical reading of the manuscript. The work was supported by a grant from the Leona M. and Harry B. Helmsley Charitable Trust (2014PG-MED001) and a U.S. National Institutes of Health grant (R01 DK123712) to NM.

Author contributions
N.M. and N.V.G. designed the study, conducted experiments, carried out data analysis, data interpretation, and drafted the manuscript. I.C.S.C. and M.D. conducted experiments and helped to draft the manuscript.

Competing interests
The authors declare no competing interests.

Additional information
Correspondence and requests for materials should be addressed to N.M.

Reprints and permissions information is available at www.nature.com/reprints.

Publisher's note Springer Nature remains neutral with regard to jurisdictional claims in published maps and institutional affiliations.